

Structural and theoretical studies of intermolecular dihydrogen bonding in $[(C_6F_5)_2(C_6Cl_5)B]-H \cdots H-[TMP]^+$

Cite this: *Chem. Commun.*, 2013, **49**, 9755

Received 1st August 2013,
Accepted 9th September 2013

DOI: 10.1039/c3cc45889j

www.rsc.org/chemcomm

The product of the intermolecular ‘frustrated Lewis pair’ (FLP) $B(C_6F_5)_2(C_6Cl_5)/2,2,6,6$ -tetramethylpiperidine and H_2 has been studied by single-crystal neutron diffraction. This is the first structurally characterised example of a geometrically unconstrained dihydrogen ($H \cdots H$) bond within a hydrogenated FLP system.

In 2006, Stephan and co-workers uncovered the first metal-free system that reversibly splits H_2 .¹ They succeeded in activating H_2 using a frustrated Lewis pair (FLP), which is defined as a Lewis acid and a Lewis base that are unable to form a ‘classical’ donor–acceptor bond due to steric hindrance between the components.² Since then FLPs have been used in a variety of small molecule activation reactions, including H_2 heterolysis,³ CO_2 sequestration,⁴ and the addition of both homopolar⁵ and heteropolar⁶ unsaturated substrates. Amongst the most exciting applications of FLPs is their ability to add H_2 to bulky imines,^{5c–7} and to mediate the hydrogenation of CO_2 to CH_3OH .^{4a,8} The mechanism by which FLPs activate H_2 is still being debated; two principal models (electric field polarisation⁹ or synergistic electron transfer)¹⁰ have been proposed for how $H-H$ bond cleavage proceeds.¹¹ Free energy calculations have shown themselves to be a useful tool for predicting reversibility in H_2 cleavage by FLPs, and are considered to be a reliable tool in guiding the design of future improved FLP-mediated hydrogenation catalysts. Pápai *et al.* have correlated the thermodynamic feasibility of H_2 cleavage by FLPs with cumulative acid–base strengths, and also noted that product stabilisation (ion pair formation) plays a key contribution to the overall energetics; however, this factor was found to vary little (-14 to -24 kcal mol⁻¹)

over a wide range of intermolecular FLP systems.¹² Accurate structural data of the products of H_2 activation could assist theoretical studies by enabling one side of the reaction coordinate to be well defined. In particular, species which contain dihydrogen bonding could be useful models, since this feature has been calculated to stabilise ionic boron hydrides by up to 6.5 kcal mol⁻¹.¹³ This could have a significant impact on the reversibility of H_2 heterolysis by FLPs where ΔG has been calculated to be close to zero, on the basis of non-interacting ion pair products.

Steiner has formally categorised a “moderate/normal” dihydrogen bond as having an internuclear distance of between 1.50 and 2.20 Å.¹⁴ Curiously, DFT calculations have predicted such a feature to be present in $[(C_6F_5)_3B-H][H-P^tBu_3]$ ($P-H \cdots H-B = 1.87$ Å),^{10a} yet experimental data (X-ray) show the corresponding separation to be significantly longer (2.75 Å).¹⁵ Similarly, $[(C_6F_5)_3B-H][H-TMP]$ ($TMP = 2,2,6,6$ -tetramethylpiperidine) has been structurally characterised, and also does not contain a dihydrogen bond ($N-H \cdots H-B = 2.97$ Å).¹⁶ Conversely, Schulz *et al.* demonstrated using single crystal neutron diffraction that a hydrogen bond interaction (1.67 Å) was present upon H_2 splitting by the intramolecular FLP system 1-*N*-TMPH- CH_2 -2-[$HB(C_6F_5)_2$] C_6H_4 (**1**, Fig. 1).¹⁷ However, since this FLP system contains a bridge that forces the Lewis acidic and basic centres together, it is possible that rigid geometric factors could impact upon the $H \cdots H$ distance, and hence this may not truly reflect an unconstrained dihydrogen bond.

Recently we described the synthesis and characterisation of a series of electrophilic boranes, $B(C_6Cl_5)_x(C_6F_5)_{3-x}$ ($x = 1-3$).¹⁸ During the course of our studies into the heterolytic cleavage of H_2 with the bimolecular FLP system $B(C_6Cl_5)(C_6F_5)_2-TMP$, we isolated large single crystals of $[(C_6F_5)_2(C_6Cl_5)B-H][H-TMP]^+$ (**2**, Fig. 1), which have been characterised by multinuclear NMR, elemental analysis and MS.† The structure of **2** has been determined by single crystal X-ray diffraction studies‡ and demonstrates that after splitting H_2 , the orientation of the ion pair in the salt is consistent with a possible dihydrogen bond ($H \cdots H = 1.844(2)$ Å) between the piperidinium and borohydride moieties. However, the precise location and bond

^a Inorganic Chemistry Laboratory, University of Oxford, South Parks Road, Oxford OX1 3QR, UK. E-mail: dermot.ohare@chem.ox.ac.uk; Fax: +44 (0)1865 272690; Tel: +44 (0)1865 285130

^b Department of Chemistry, Imperial College London, South Kensington, London SW7 2AZ, UK. E-mail: a.ashley@imperial.ac.uk; Tel: +44 (0)20 759 45810

^c ISIS Facility, Rutherford Appleton Laboratory-STFC, Chilton, Didcot, Oxford OX11 0QX, UK

† Electronic supplementary information (ESI) available. CCDC 953644 and 953645. For ESI and crystallographic data in CIF or other electronic format see DOI: 10.1039/c3cc45889j

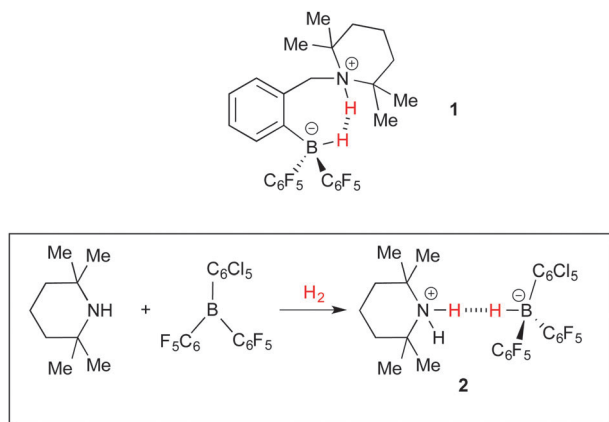


Fig. 1 Crystallographically characterised products of FLP-mediated H_2 cleavage which demonstrate dihydrogen bonds. Top: intramolecular example reported by Schulz *et al.*¹⁷ bottom: synthesis of the intermolecular system, $[(C_6F_5)_2(C_6Cl_5)B-H][H-TMP]$, **2**.

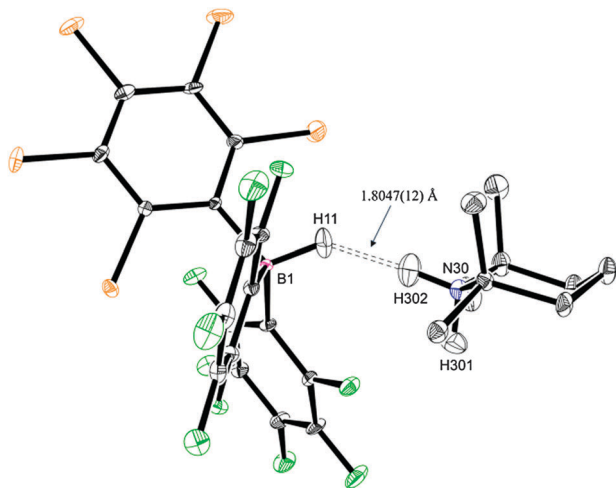


Fig. 2 Neutron structure of $[(C_6F_5)_2(C_6Cl_5)B-H][H-TMP]$ (**2**) at 100 K. Thermal ellipsoids at 50% probability. H atoms on the TMP molecule (except those bound to N atom) have been omitted for clarity.

distance between the hydrogen nuclei could not be adequately resolved by X-ray diffraction, and in order to accurately determine the geometry of B-H \cdots H-N unit, we resorted to a single crystal neutron diffraction measurement (Fig. 2).

For comparative purposes, the electronic structure of **2** was also explored and optimised using density functional theory (DFT; B97D/TZVP), and pertinent metric data for all techniques are collated in Table 1.

In general, the neutron structure agrees well with the X-ray structure, displaying a four-coordinate boron atom which adopts a *pseudo*-tetrahedral coordination geometry. However, the H \cdots H distance (1.8047(12) Å) is noticeably shorter than that determined by X-ray diffraction and DFT calculations, yet is substantially longer than the interhydrogen distance in free H_2 (0.74 Å) or non-classical H_2 transition metal complexes (*ca.* 0.82 Å).¹⁹ The geometry of the B-H \cdots H-N fragment is also bent, as revealed by the B-H \cdots H(N) bond angle. This is reported to be a common structural feature of dihydrogen bonding, and Crabtree has

Table 1 Comparison of selected bond lengths and angles for **2**, as determined by single crystal X-ray and neutron diffraction, and calculated data (B97-D/TZVP). H atom numbering scheme applies to atom connectivity shown in Fig. 2

	Experimental X-ray [§]	Experimental neutron [§]	Calculated ^a
H(11) \cdots H(302) (Å)	1.844(2)	1.8047(12)	1.867
N-H(301) (Å)	0.897	1.030(8)	1.024
N-H(302) (Å)	0.882	1.038(9)	1.032
B-H(11) (Å)	1.353	1.203(9)	1.223
B-H(11) \cdots H(302) (°)	136.43(5)	139.5(8)	127.5
N-H(302) \cdots H(11) (°)	174.95(5)	174.4(9)	152.1

^a Performed using a polarisable continuum model (PCM) with the dielectric constant corresponding to that of water ($\epsilon = 78.4$), in order to mimic the electric field within the crystalline lattice.

studied the solid-state structure of H_3N-BH_3 , where it is reported that various intermolecular H \cdots H contacts (range 1.7–2.2 Å) have N-H \cdots H-B bond angles which are appreciably larger than B-H \cdots H-N, which is also seen in the structure of **2**.²⁰

Furthermore, calculations on the ammonia borane dimer have shown that the B-H \cdots H-N bond strength is 6.1 kcal mol⁻¹, which would confer appreciable energetic stability to species containing this moiety. This could have an effect on the reversibility of FLP H_2 heterolysis; interestingly, **2** shows no loss of H_2 in the solid state upon heating *in vacuo* (18 hours, 110 °C, 10⁻² mbar). Furthermore, X-ray data appreciably underestimate the N-H bond lengths, whereas the converse is true for B-H, relative to the neutron results. Overall, with respect to the B-H \cdots H-N unit, DFT calculations for **2** correspond more closely with the experimental neutron structure than X-ray data. The Wiberg bond index for the dihydrogen bond in **2** of 0.011 (Table S1, ESI[†]) is indicative of significant interaction between the two participating hydrogen atoms. This value is larger compared to the bond orders of the closest H \cdots X interactions between fragments in the dimer. For comparison we calculate a bond index of 0.022 for the stronger H \cdots H interaction in the ammonia borane dimer.

The B-H and N-H bond lengths (1.24 and 1.03 Å respectively)¹⁷ for **1** reported by Schulz *et al.* are comparable to those determined for **2**. However, the distance between the H atoms for the former is significantly shorter than that seen in **2**. One explanation for this observation could be that the bridge between the borate and N-base fragments in 1-*N*-TMPH-CH₂-2-[HB(C₆F₅)₂]C₆H₄ provides limited flexibility to accommodate the H \cdots H interaction, which is supported by an internuclear B \cdots N separation of 3.35 Å, compared to the significantly larger 3.829(3) Å seen in intermolecular **2**.

The X-ray and neutron structure of $[(C_6F_5)_2(C_6Cl_5)B-H][H-TMP]$ show that the H atoms from FLP-mediated H_2 heterolysis are contained within a non-linear B-H \cdots H(N) fragment. Single crystal neutron diffraction data allows the precise position of the H atoms to be determined, revealing the presence of a short B-H \cdots H-N dihydrogen bond linking the ion pair. This is the first dihydrogen bond to be reported for the product of H_2 cleavage by an intermolecular FLP.

Notes and references

[†] Synthesis of $[(C_6F_5)_2(C_6Cl_5)B-H][H-TMP]$ (**2**): a 50 ml thick-walled glass ampoule was charged with a magnetic stir bar, B(C₆Cl₅)(C₆F₅)₂ (ref. 18) (0.30 g, 0.84 mmol), TMP (118 mg, 0.84 mmol) and anhydrous

toluene (15 ml) under N₂. The reaction was freeze-pump-thaw degassed three times with H₂ (1 atm), sealed at room temperature, and then heated (110 °C) for 7 days with stirring. The solvent was removed under vacuum and the residue was washed with pentane (2 × 10 ml), the solids collected and dried under vacuum (10⁻² mbar) at 80 °C to afford 2 as a colourless solid (284 mg, 76%, 0.38 mmol). ¹H NMR (CD₃CN, 300 MHz): δ 6.21 (t (1:1:1), 2H, ¹J_{NH} = 51 Hz, NH₂); 3.81 (q (1:1:1:1:1), 1H, ¹J_{BH} = 90 Hz, BH); 1.73 (m, 2H, CH₂, TMP); 1.63 (m, 4H, CH₂, TMP); 1.39 (s, 12H, CH₃, TMP). ¹¹B NMR (CD₃CN, 128 MHz): δ -19.8 (d, ¹J_{BH} = 90 Hz). ¹³C{¹H} NMR (CD₃CN, 75 MHz): δ 149.5 (dm, ¹J_{CF} = 234 Hz, *ortho*-C₆F₅); 145.0 (br s, *ipso*-C₆Cl₅); 139.3 (s, *ipso*-C₆Cl₅); 139.0 (dm, ¹J_{CF} = 242 Hz, *para*-C₆F₅); 137.90 (dm, ¹J_{CF} = 243 Hz, *meta*-C₆F₅); 131.3 (s, *para*-C₆Cl₅); 129.8, 126.2 (both s, *meta*-C₆Cl₅ and *ortho*-C₆Cl₅); 126.16 (br s, *ipso*-C₆F₅); 59.76 (s, NC(CH₃)₂CH₂); 35.73 (s, NC(CH₃)₂CH₂); 27.68 (s, NC(CH₃)₂CH₂); 17.01 (s, NC(CH₃)₂-CH₂CH₂); *ipso*-C₆F₅ was not observed. ¹⁹F NMR (CD₃CN, 282 MHz): δ -134.5 (d, 4F, ³J_{FF} = 22 Hz, *ortho*-C₆F₅); -165.3 (t, 2F, ³J_{FF} = 19 Hz, *para*-C₆F₅); -168.4 (m, 4F, *meta*-C₆F₅). HRMS (ESI⁻, *m/z*): for C₁₈HBCl₁₀F₅ calcd: 592.8471. Found: 592.8471. IR (cm⁻¹): 2959 (w), 2262 (w), 1639 (w), 1573 (s), 1512 (s), 1452 (s), 1384 (s), 1327 (w), 1301 (s), 1259 (s), 1076 (m), 958 (s), 893 (s), 785 (s). Anal. calcd for C₂₇H₂₁BCl₅F₁₀N: C 43.97; H 2.87; N 1.90. Found: C 44.07; H 2.78; N 2.04.

§ Single crystals for both X-ray and neutron diffraction were grown from a saturated toluene solution of 2, which was layered with pentane (298 K). Single crystal X-ray diffraction data were collected at 100 K with an Oxford Diffraction (Agilent) SuperNova diffractometer. Data collection, unit cell refinement, integration, interframe scaling and absorption corrections were carried out using CrysAlisPro. The structure was solved with SuperFlip²¹ and refined with CRYSTALS.²² Neutron diffraction data were collected at 100 K using the time-of-flight Laue diffractometer SXD at the ISIS spallation neutron source.²³ The structure from the X-ray solution was refined against the neutron diffraction data, using SHELXTL.²⁴ Full refinement details for both datasets are given in the ESI[†] CCDC 953644 and 953645. Single crystal diffraction data: C₂₇H₂₁BCl₅F₁₀N, *M_r* = 737.52, monoclinic, *P*₂₁/*c*, *Z* = 4, *T* = 100 K. X-ray refinement - *a* = 14.0366(2) Å, *b* = 17.3755(2) Å, *c* = 13.3392(2) Å, β = 114.9580(17)°, *V* = 2949.53(8) Å³, data/restraints/parameters - 6171/0/397, *R*_{int} = 0.029, final *R*₁ = 0.0270, *wR*₂ = 0.0668 (*I* > -3σ(*I*)). Neutron refinement - *a* = 14.011(3) Å, *b* = 17.343(4) Å, *c* = 13.332(3) Å, β = 115.030(15)°, *V* = 2935.5(11) Å³, data/restraints/parameters - 14355/0/596, final *R*₁ = 0.0928, *wR*₂ = 0.2584 (all data).

- 1 G. C. Welch, R. R. S. Juan, J. D. Masuda and D. W. Stephan, *Science*, 2006, **314**, 1124.
- 2 G. C. Welch, L. Cabrera, P. A. Chase, E. Hollink, J. D. Masuda, P. R. Wei and D. W. Stephan, *Dalton Trans.*, 2007, 3407.
- 3 D. W. Stephan and G. Erker, *Angew. Chem., Int. Ed.*, 2010, **49**, 46.

- 4 (a) A. E. Ashley, A. L. Thompson and D. O'Hare, *Angew. Chem., Int. Ed.*, 2009, **48**, 9839; (b) G. Menard and D. W. Stephan, *J. Am. Chem. Soc.*, 2010, **132**, 1796; (c) X. Zhao and D. W. Stephan, *Chem. Commun.*, 2011, **47**, 1833.
- 5 (a) A. Stirling, A. Hamza, T. A. Rokob and I. Papai, *Chem. Commun.*, 2008, 3148; (b) A. Stute, G. Kehr, R. Frohlich and G. Erker, *Chem. Commun.*, 2011, **47**, 4288; (c) M. L. Ullrich, A. J. Lough and D. W. Stephan, *Organometallics*, 2010, **29**, 3647.
- 6 C. M. Momming, E. Otten, G. Kehr, R. Frohlich, S. Grimme, D. W. Stephan and G. Erker, *Angew. Chem., Int. Ed.*, 2009, **48**, 6643.
- 7 (a) P. A. Chase, G. C. Welch, T. Jurca and D. W. Stephan, *Angew. Chem., Int. Ed.*, 2007, **46**, 8050; (b) P. A. Chase, T. Jurca and D. W. Stephan, *Chem. Commun.*, 2008, 1701; (c) D. Chen, Y. Wang and J. Klankermayer, *Angew. Chem., Int. Ed.*, 2010, **49**, 9475.
- 8 M. J. Sgro, J. Domer and D. W. Stephan, *Chem. Commun.*, 2012, **42**, 7253.
- 9 S. Grimme, H. Kruse, L. Goerigk and G. Erker, *Angew. Chem., Int. Ed.*, 2010, **49**, 1402.
- 10 (a) T. A. Rokob, A. Hamza, A. Stirling, T. Soós and I. Pápai, *Angew. Chem., Int. Ed.*, 2008, **47**, 2435; (b) A. Hamza, A. Stirling, T. András Rokob and I. Pápai, *Int. J. Quantum Chem.*, 2009, **109**, 2416.
- 11 T. A. Rokob, I. Bakó, A. Stirling, A. Hamza and I. Pápai, *J. Am. Chem. Soc.*, 2013, **135**, 4425.
- 12 T. A. Rokob, A. Hamza and I. Pápai, *J. Am. Chem. Soc.*, 2009, **131**, 10701.
- 13 R. Custelcean and J. E. Jackson, *Chem. Rev.*, 2001, **101**, 1963.
- 14 T. Steiner, *Angew. Chem., Int. Ed.*, 2002, **41**, 48.
- 15 G. C. Welch and D. W. Stephan, *J. Am. Chem. Soc.*, 2007, **129**, 1880.
- 16 V. Sumerin, F. Schulz, M. Nieger, M. Leskel, T. Repo and B. Rieger, *Angew. Chem., Int. Ed.*, 2008, **47**, 6001.
- 17 F. Schulz, V. Sumerin, S. Heikkinen, B. Pedersen, C. Wang, M. Atsumi, M. Leskelä, T. Repo, P. Pyykkö, W. Petry and B. Rieger, *J. Am. Chem. Soc.*, 2011, **133**, 20245.
- 18 A. E. Ashley, T. J. Herrington, G. G. Wildgoose, H. Zaher, A. L. Thompson, N. H. Rees, T. Kramer and D. O'Hare, *J. Am. Chem. Soc.*, 2011, **133**, 14727.
- 19 D. M. Heinekey and W. J. Oldham, *Chem. Rev.*, 1993, **93**, 913.
- 20 T. B. Richardson, S. de Gala, R. H. Crabtree and P. E. M. Siegbhan, *J. Am. Chem. Soc.*, 1995, **117**, 12875.
- 21 L. Palatinus and G. Chapuis, *J. Appl. Crystallogr.*, 1997, **40**, 786.
- 22 P. W. Betteridge, J. R. Carruthers, R. I. Cooper, K. Prout and D. J. Watkin, *J. Appl. Crystallogr.*, 2003, **36**, 1487; R. I. Cooper, A. L. Thompson and D. J. Watkin, *J. Appl. Crystallogr.*, 2010, **43**, 1100.
- 23 D. A. Keen, M. J. Gutmann and C. C. Wilson, *J. Appl. Crystallogr.*, 2006, **39**, 714.
- 24 G. M. Sheldrick, *Acta Crystallogr., Sect. A*, 2008, **64**, 112.